Supporting Information for

Strong Dual Emission in Covalent Organic Frameworks Induced by ESIPT

Hua-Qing Yin[a], Fangfei Yin[a], Xue-Bo Yin*[a]

[1]State Key Laboratory of Medicinal Chemical Biology, Tianjin Key Laboratory of Biosensing and Molecular Recognition, College of Chemistry, Nankai University, Tianjin

Email: xbyin@nankai.edu.cn

Table of Contents

Section 1. Materials

1,3,5-Triformylbenzene (TFB), 2,4,6-triformylphloroglucinol (TFP), 9,9-dibutyl-2,7-diaminofluorene (DDAF), and 9,9-dioctyl-2,7-diaminofluorene (DOAF) were obtained from Haoyu Chemical Technology Co. Ltd (Hangzhou, China). 2,7-Diamiofluorene (DAF) was bought from Yuanye Biotechnology Co. Ltd (Shanghai, China). Salicylaldehyde and benzaldehyde were obtained from Energy Chemical Co. Ltd (Shanghai China). Disodium hydrogen phosphate and sodium dihydrogen phosphate were obtained from Fuchen Chemical Regents Factory (Tianjing, China). N, N-dimethylformamide, 1,4-dioxane, acetone, and ice acetic acid were purchased from Concord Chemical Research Institute (Tianjin, China). All chemicals and reagents used were at least of analytical grade. Super dry dimethyl sulfoxide, methanol, and ethanol with molecular sieves were purchased from J&K scientific Co. Ltd. (Beijing, China). Ultrapure water was prepared with an Aquapro system (18.25 MΩ cm).

Section 2. Instrumentations

UV-Vis absorption spectrum was recorded by a UV-3900-visible spectrophotometer, Hitachi, Japan. The steady-state fluorescence experiments were performed on a FL-4600 Fluorescence Spectrometer, Hitachi, Japan, equipped with a plotter unit and a quartz cell (1 cm × 1 cm). Fourier transform infrared spectra (FTIR) were obtained by Bruker TENSOR 27 Fourier transform infrared spectroscopy. Thermogravimetric analysis (TGA) was performed on a PTC-10ATG-DTA analyzer heated from 20 °C at a ramp rate of 15 °C min^{-1} under air. Transmission electron microscopy (TEM) images were recorded with TecnaiG2 F20, FEI Co. (America) operated at an accelerating voltage of 200 kV. Scanning Electron Microscopy (SEM) images were obtained with JSM-7500F, Japan. N_2 adsorption-desorption isotherm was recorded with ASAP2020/Tristar 3000 surface area and pore analyzer at 274 K. PXRD patterns were obtained on a D/max-2500 diffractometer (Rigaku, Japan) using Cu K radiation (λ = 1.5418 Å) with a scanning speed of 8° min^{-1} and a step size of 0.02° in 2θ. Solid-state NMR experiments were performed on Infinity plus 300, Varian, America. Elemental analysis was carried out on a vario EL CUBE analyzer (Elementary, Germany). N_2 adsorption-desorption isotherms and the pore size distribution were tested by on the

NOVA 2000e surface area and pore size analyzer at 77K. The pore-size distribution has been calculated by BJH method according to the DFT program. Quantum yield measurement was performed by the Hamamatsu absolute PL quantum yield spectrometer C11347 (Hamamatsu, Japan). Solid and solution state emission spectra were recorded using Fluoro Max-4 spectrophotometer (Horiba Jobin Yvon, USA) equipped with the solid-state sample holder.

Section 3. Synthesis Methods

3.1 Synthesis of COF-4-OH

The COFs prepared with DDAF and TFP was denoted as COF-4-OH, where "4" represented the butyl groups and "–OH" was the hydroxyl group. A 20 mL glass vial was added with TFP (15 mg, 0.065mmol), aniline (0.102 mL, 1.125 mmol), and 0.5 mL of 1,4-dioxane, then 0.2 mL of 6 M acetic acid was added to the mixed solution. DDAF (33mg, 0.11 mmol) dissolved in 1,4-dioxane (0.5 mL) was then added. After 10 min of sonication, the mixture was allowed to further stand at ambient temperature for 60 days. The as-formed orange product was collected via filtration and rinsed with 1, 4-dioxane and acetone. The as-synthesized products were immersed in acetone for 24 h to exchange the guest molecules in the pores and dried at 100 °C under vacuum for 24 h to obtain COF-4-OH with ca. 85.0% yield. Fourier transform-infrared spectroscopy (FTIR): 3370, 3304, 3200, 2928, 2847, 1614, 1441, 1241, 1088, 985, and 801 cm^{-1}. Elemental analysis of $(C_{13.5}H_{14}NO)_n$ is C, 78.64; H, 6.80; and N, 6.80, while C, 76.53; H, 6.60; and N, 7.10 were found. The peaks at 5.03°, 7.62°, 10.50°, and 11.68° were observed at its Powder X-ray diffraction (PXRD).

COF-4-OH also can be obtained by the solvothermal method. A 10 mL pyrex tube was added with TFP (15 mg, 0.065mmol), and 0.5 mL of 1,4-dioxane, then 0.2 mL of 6 M acetic acid was added to the mixed solution. DDAF (33mg, 0.11 mmol) dissolved in 1,4-dioxane (0.5 mL) was then added. After 30 seconds of sonication, the mixture degassed through three freeze–pump–thaw cycles, sealed under vacuum, and heated at 120 °C for 5 days. The as-formed orange product was collected via filtration and rinsed with 1, 4-dioxane and acetone.

3.2 Synthesis of COF-0-OH and COF-8-OH

COF-0-OH and COF-8-OH were prepared in the same way as COF-4-OH by replacing

DDAF with DAF (12.7mg, 0.065mmol) or DOAF (15mg, 0.065mmol). The as-synthetic COF-0-OH and COF-8-0H was in ca. 90.5% and 50.2% isolated yield. FTIR spectrum of COF-0-OH: 3377, 3304, 3206, 3009, 1610, 1465, 1323, 1242, 1119, 800, and 690 cm^{-1}. Elemental analysis of $(C_{11}H_7NO)_n$: C 78.11%, H 4.14%, and N 8.28%, while C 77.09%, H 4.24%, and N 8.47% were found. The peaks at 3.45°, 5.94° and 6.89° was observed in COF-0-OH PXRD pattern.

3.3 Synthesis of COF-4 and COF-0

COF-4 was prepared in the same way as COF-4-OH by replacing TFP with TFB (21.6 mg, 0.13 mmol). COF-0 prepared according to the literature.[1] The COF-4 was obtained in ca.71.2 % isolated yield. FTIR of COF-4: 2923, 2858, 1699, 1606, 1461, 1372, 1134, 962, 812, and 678 cm^{-1}. Elemental analysis of $(C_{13.5}H_{14}N)_n$: C 85.26%, H 7.37%, and N 7.37%, while C 86.19%, H 7.17%, and N 7.24% were found. No obviously characteristic peak was observed in its PXRD pattern.

3.4 Synthesis of Model 1

After DDAF (1.5 mg, 0.01 mmol) was dissolved in 1.5 mL of DMF, 0.02 mL of salicylaldehyde (0.02 mmol) and 0.05 mL of 6 M acetic acid aqueous were added in the solution. After sonication 10 min, the mixture was refluxed for 24 h, and yellow production was collected.

3.5 Synthesis of Model 2 and 3

Model 2 was prepared in the same way as Model 1 by replacing salicylaldehyde with benzaldehyde (0.02 mg, 0.02 mmol). Model 3 was prepared in the same way as Model 1 by replacing DDAF with DAF (0.02 mg, 0.02 mmol).

Section 4. Analysis Methods

4.1 Structural Simulation and PXRD Analysis

Structure Modeling of COF-4-OH was conducted with the Material Studio (v. 7.0) suite of program by Accelrys. The initial lattice was generated with the space group P1 (a=b=30.0000 Å, c=5.0000 Å), and the unit cell was defined by two DDAF molecules bonded to TFP via six hydrazine linkages. After geometry optimization using the Material Studio Forcite

molecular module (Universal force fields, Ewald summations), the crude structure Modeling of COF-4-OH was obtained. Subsequently, Pawley refinement was applied to obtain the refined PXRD profile with the lattice parameters a=b=29.2482 Å, c=5.5320 Å, and Rwp value of 9.45% and Rp value of 6.53% were obtained. An AB staggered arrangement for COF-4-OH as an alternative structure was performed wherein the initial lattice was generated with the space group P1 (a=b=29.2842 Å, c=5.5320 Å).

4.2 Interlayer Spacing Measurement

For interlayer spacing measurement of the COFs, the lattice model was optimized using the Materials Studio (v.7.0) Forcite calculation modules energy, geometry optimization, and dynamics calculation, under universal force fields, utra-fine condition. Then Pawley refinement was performed to optimize the lattice parameters until the Rwp value converged. The interlayer spacing was measured by the distance tool used the diamond (v.3.2) between the (001) plane for COF-4-OH and COF-8-OH and (011) plane for COF-0-OH.

4.3 Time dependent Density Functional Theory (TD-DFT)

Theoretical optical properties were tested using Time dependent Density Functional Theory (TD-DFT) implemented in the software Gaussian 09 employing a b3lyp functionality. The standard 6–31G (d.p) basis set of double split valence plus polarization functions on H atoms was chosen. A fix number of 25 states were selected for a proper comparison between all configurations and models.

4.4 Quantum Yield Measurement

The quantum yield (QY) of the COFs was measured in solid state with sodium salicylate as reference. Under the excitation of 280 nm, pure sodium salicylate were firstly detected. Then, about 20 mg of the COFs were added into to the circular quartz cell to detect the QY for three times.

The QY of three models was detected in liquid state with DMF as a solvent. Under the suitable excitation, the pure DMF as reference was tested firstly. Then, 0.02 mL model solution was added into DMF to get dilute solution for QY measurement for three times.

4.5 Fluorescence Lifetime Fitting

The analysis of the lifetime data was using IBH DAS6 analysis software. The bi-exponential emission decay profile was calculated by using the following fitting function:

$$R_{(t)} = A1 + B1e^{-t/\tau 1} + B2e^{-t/\tau 2}$$

Here, A_1 is the noise background, τ_i are the pre-exponential factor and fluorescence lifetime for the i^{th} component, respectively. The excellence of each bi-exponential fitting was judged by χ^2 values and the visual inspection of the residuals. The χ^2 is defined as followed:

$$\chi^2 = \frac{1}{N}\sum_{k=1}^{N}\left[\frac{I(tk) - F(tk)}{\sigma(k)}\right]^2$$

Here, $I(t_k)$ is the fluorescence decay data, $F(t_k)$ is the fitting function and $\sigma(k)$ is the standard deviation. The value of $\chi^2 \approx 1$ is considered as best fit for the plots.

4.6 Ratiometric fluorescence differentiation of organic solvents

1.0 mg of COF-4-OH was added in 20 mL of different solvents. After 5 min sonication, the above solution was added into a clean quartz cell (1×1 cm). The fluorescence spectra were recorded upon the excitation at 280 nm for the fluorescent differentiation of solvents. All of the fluorescent measurement was carried with the help of the glass filter to prevent the second harmonic peak.

4.7 Ratiometric fluorescence detection of water content in organic solvents

1.0 mg COF-4-OH was ultrasonically dispersed in 1 mL of organic solvents. 0.1 mL of the solution was added into the samples with different water contents (the total volume is 2.0 mL) in a clean plastic tube. After 10 min ultrasonic, the solution was transferred to quartz cell (1×1 cm). The fluorescence spectra were recorded upon the excitation at 280 nm for ratiometric fluorescence detection of water content.

4.8 The pH detection with COF-4-OH as probe

2.0 mg COF-4-OH was ultrasonically dispersed in 2.0 mL of organic solvent or water. The 0.1 mL solution was added to the samples with different pH (total solution volume is 2.0

mL). After about 1 min, the solution was transferred into a clean quartz cell (1×1 cm) to record the fluorescence under 280 nm excitation.

Section 5. Figures and Tables

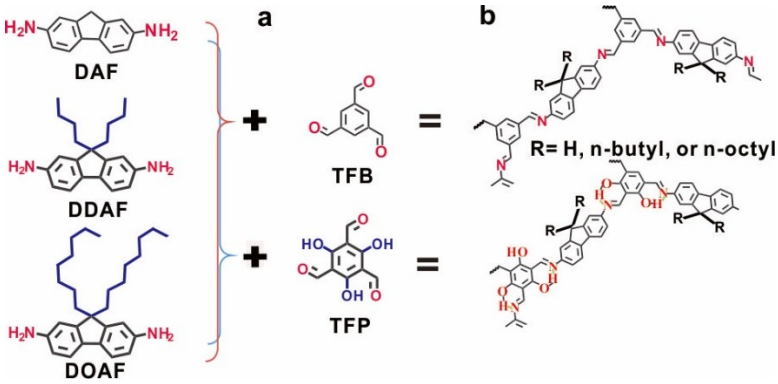

Figure S1. The design of COFs to reveal the effect of hydroxyl and alkyl groups. (a) Hydroxyl- and alkyl-groups functional monomers. (b) COFs fragments with or without hydroxyl and alkyl groups.

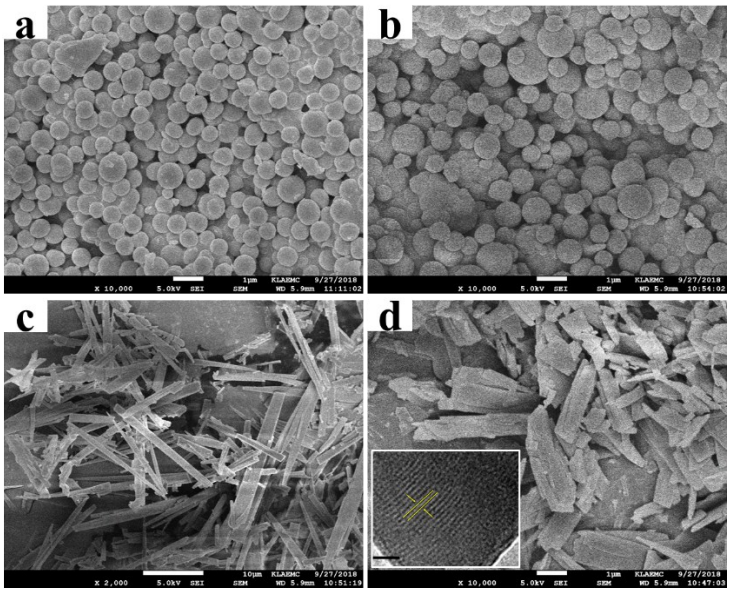

Figure S2. The SEM images of (a) COF-0, (b) COF-4, (c) COF-0-OH, and (d) COF-4-OH (Inset: high resolution TEM image of COF-4-OH).

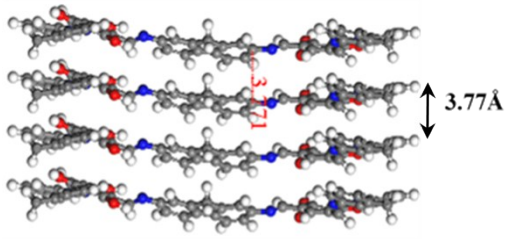

Figure S3. The layer distance of COF-0-OH.

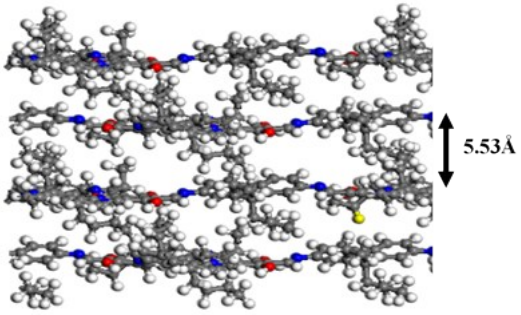

Figure S4. The layer distance of COF-4-OH.

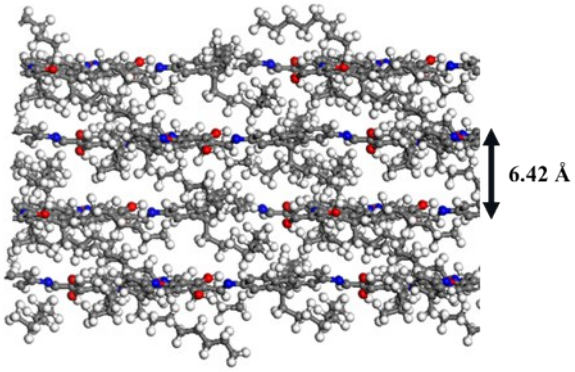

Figure S5. The layer distance of COF-8-OH.

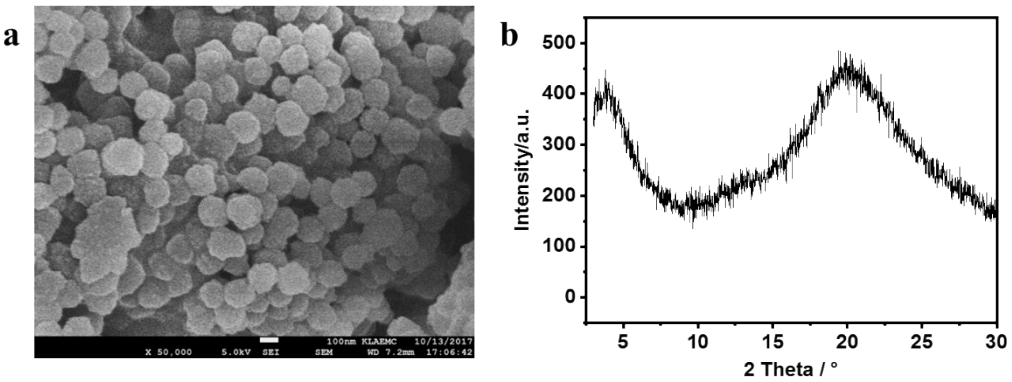

Figure S6. (a) SEM image and (b) PXRD pattern of COF-8-OH.

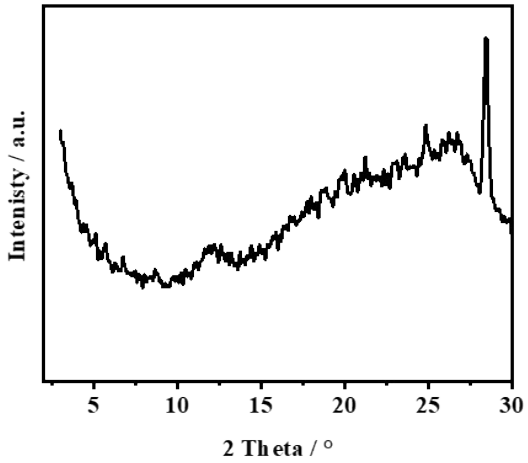

Figure S7. PXRD pattern of COF-4.

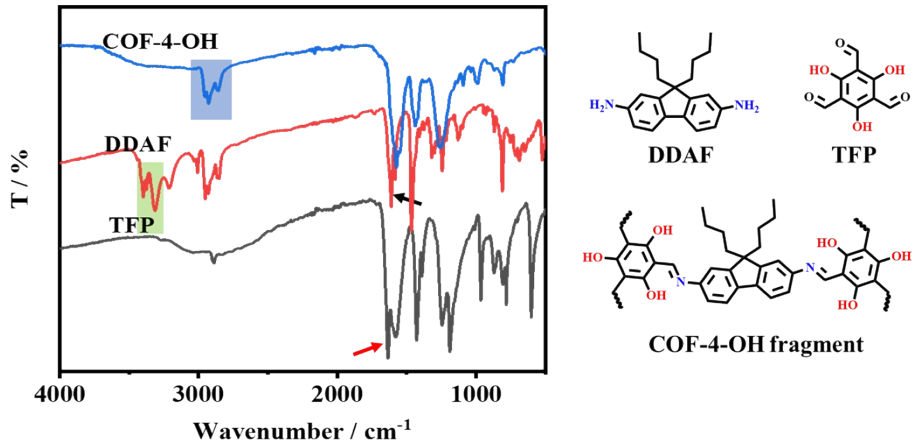

Figure S8. Fourier transform infrared (FTIR) spectra and structures of TFP, DDAF, and COF-4-OH.

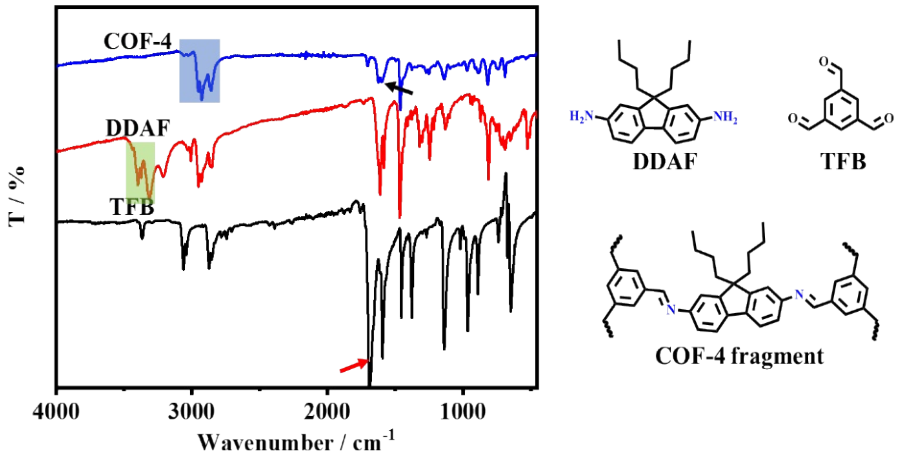

Figure S9. FTIR spectra and structures of TFB, DDAF, and COF-4.

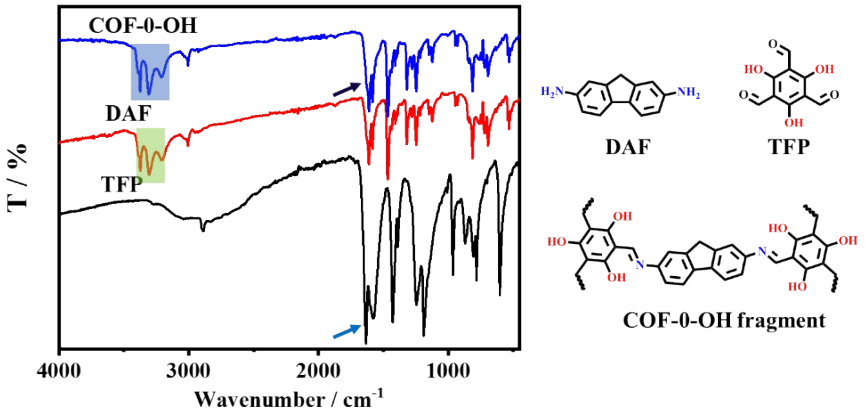

Figure S10. FTIR spectra and structures of TFP, DAF, and COF-0-OH.

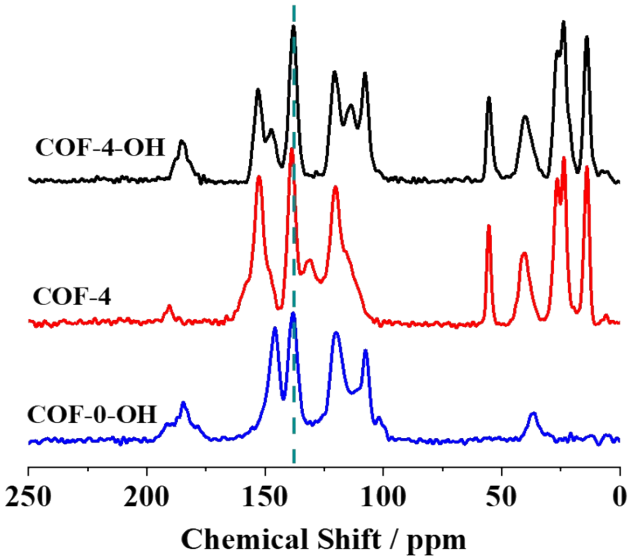

Figure S11. Solid-state ^{13}C NMR spectra of COF-4-OH, COF-4 and COF-0-OH.

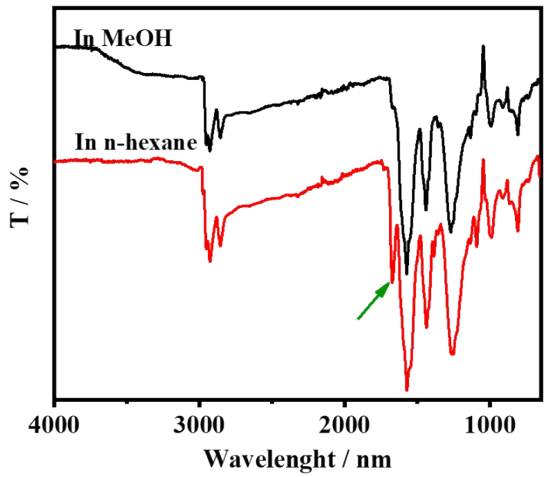

Figure S12. The FTIR spectra of COF-4-OH after soaked in methanol and *n*-hexane.

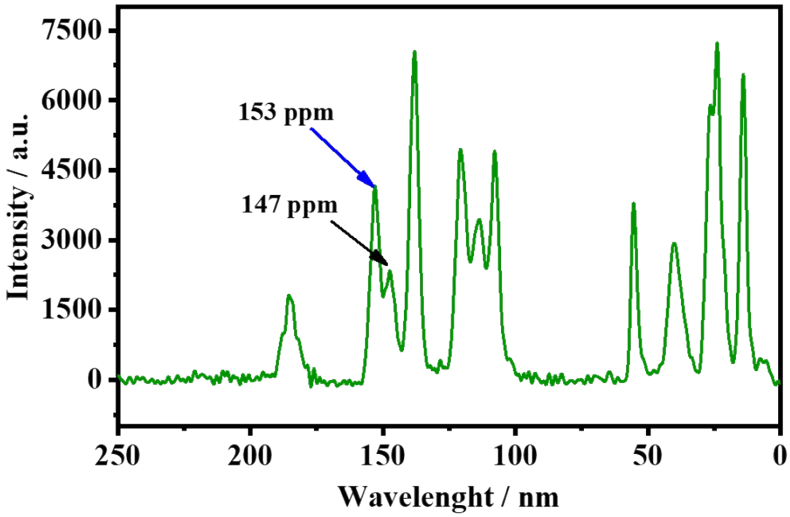

Figure S13. The solid-state ^{13}C NMR spectrum of COF-4-OH for the identification keto state at 147 ppm and enol state at 153 ppm.

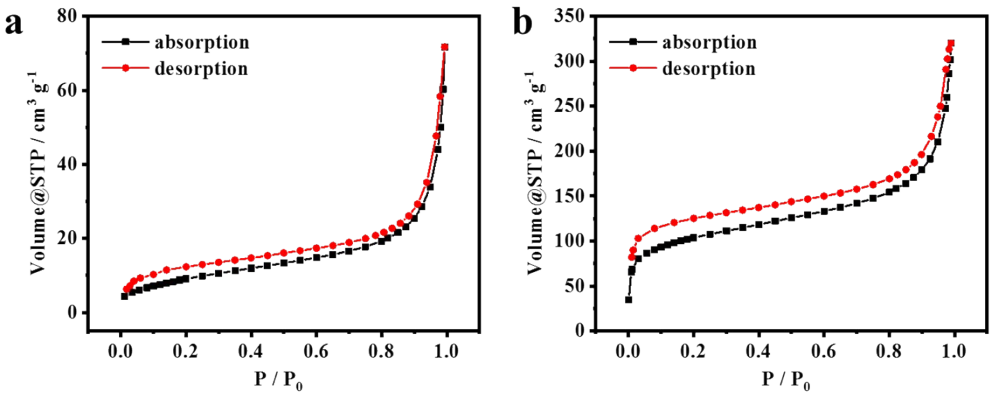

Figure S14. N_2 absorption and desorption isotherm of (a) COF-4-OH and (b) COF-0-OH.

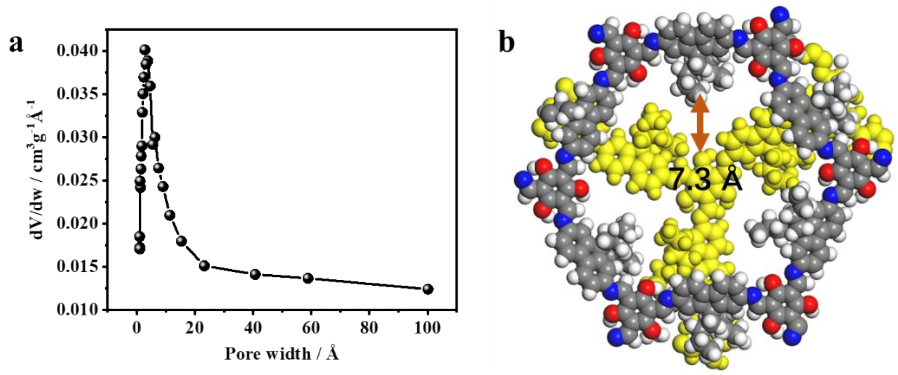

Figure S15. The pore size of COF-4-OH (a) from BET and (b) stimulated by Material Studio.

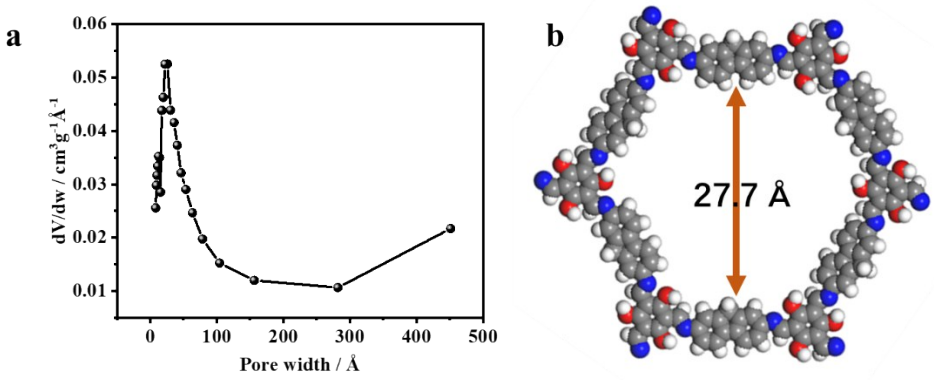

Figure S16. The pore size of COF-0-OH (a) from BET and (b) stimulated by Material Studio.

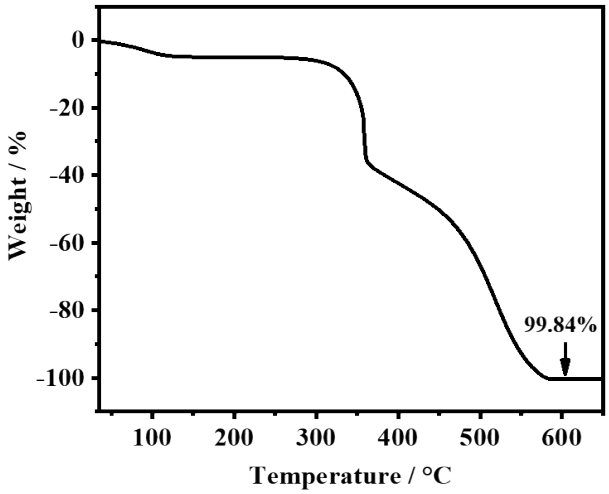

Figure S17. Thermogravimetric (TG) analysis of COF-4-OH.

Figure S18. TG analysis of COF-0-OH.

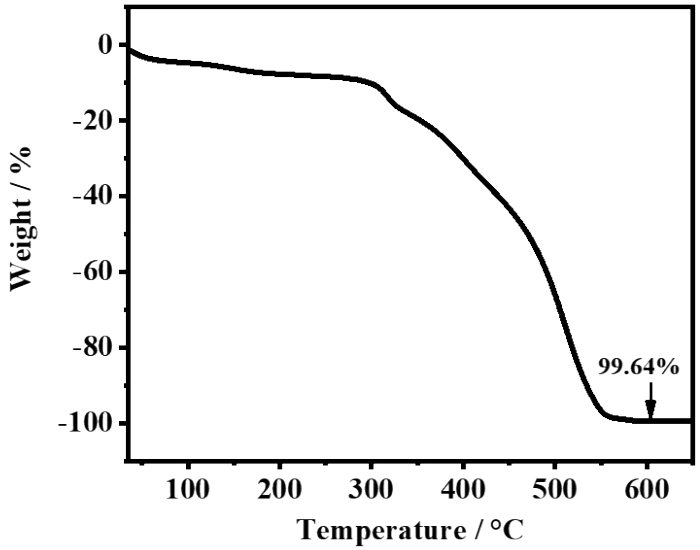

Figure S19. TG analysis of COF-4.

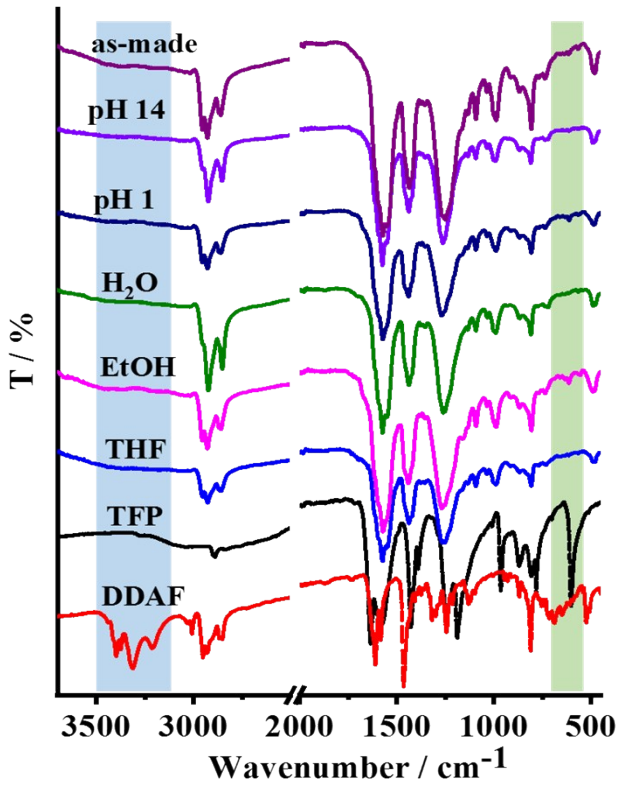

Figure S20. FTIR spectra of COF-4-OH after dispersed in different solvents for 24 h.

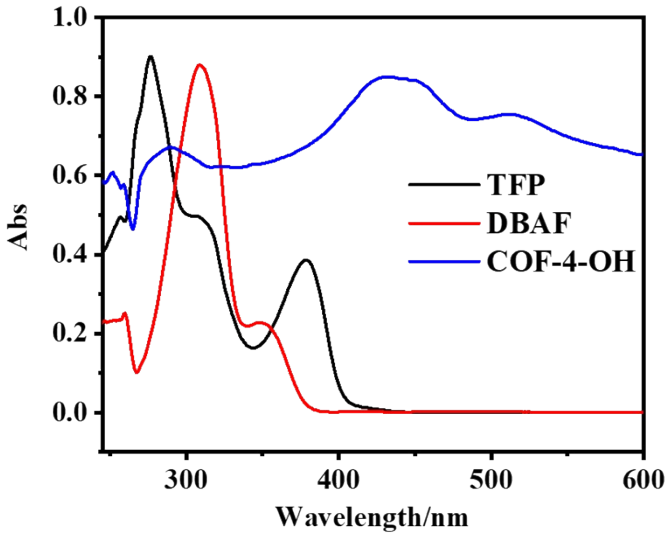

Figure S21. The UV-Vis absorption spectra of TFP, DDAF, and COF-4-OH.

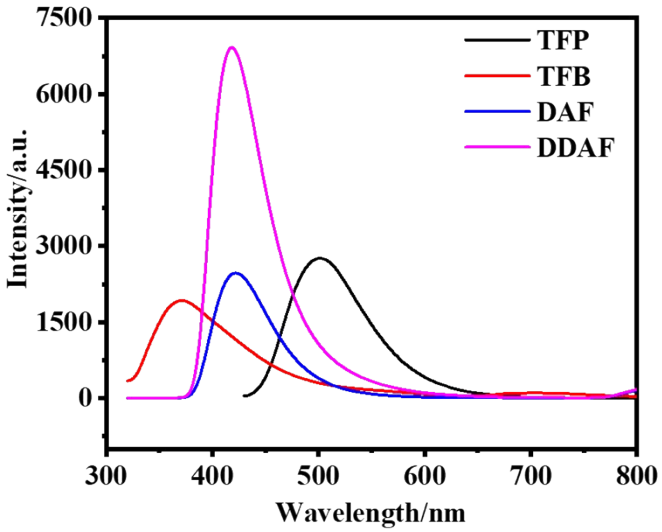

Figure S22. Fluorescence spectra of 10 μM monomers, DAF, DDAF, TFB, and TFP in DMF with their optimal excitation: TFP at 420 nm, and TFB, DDAF, and DAF at 300 nm, respectively.

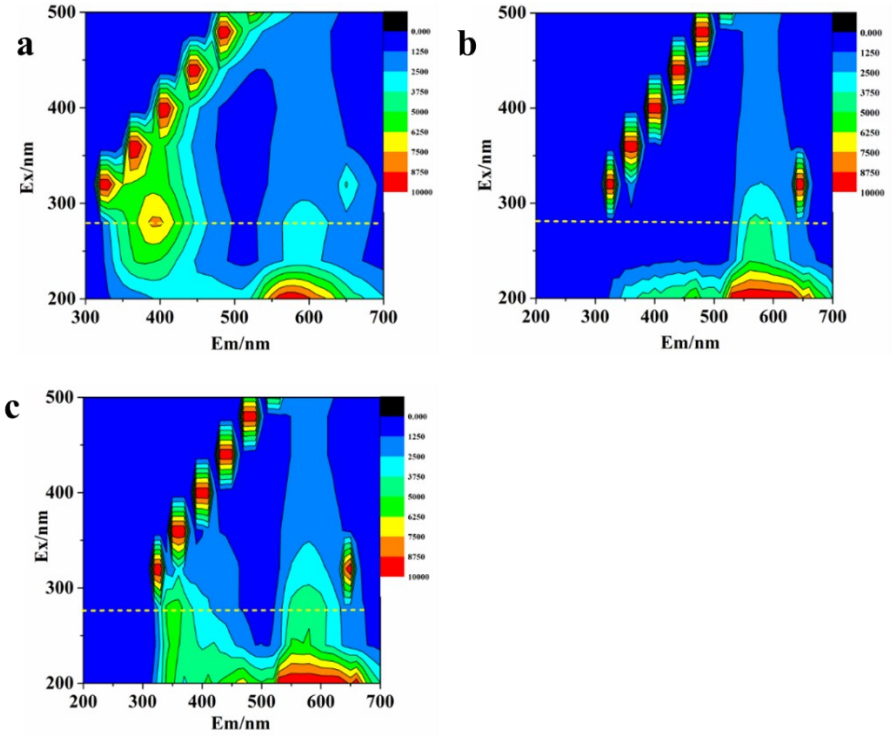

Figure S23. 3D fluorescence mapping of COF-4-OH in (a) pure ethanol, (b) pure water and (c) the mixture of water and ethanol (1:1 *v/v*). 280 nm was selected as the excitation wavelength for COF-4-OH.

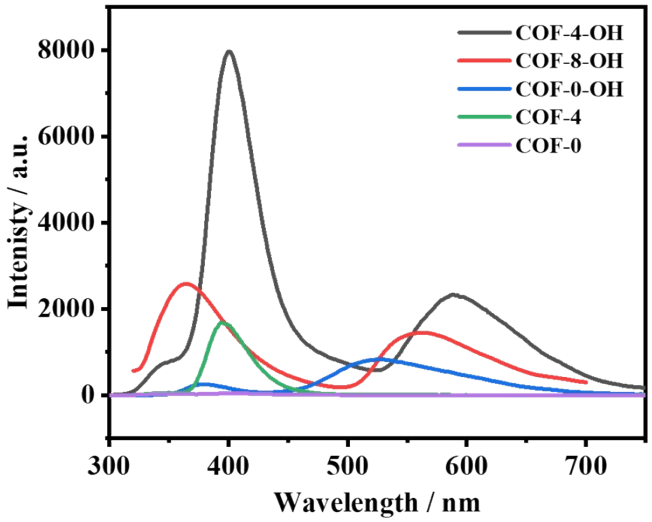

Figure S24. Fluorescence spectra of COF-4-OH, COF-8-OH, COF-0-OH, COF-4, and COF-0 at the same concentration (0.05 mg mL^{-1}) in DMF.

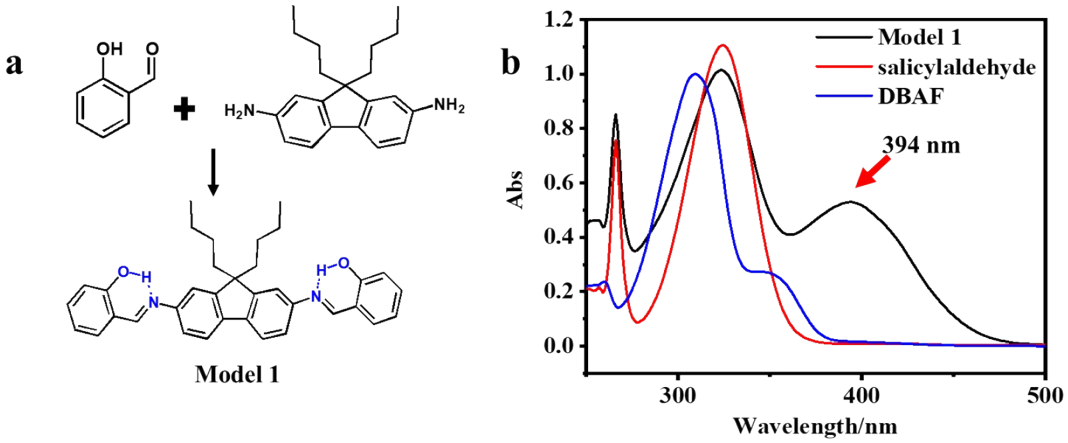

Figure S25. (a) Synthesis of Model 1 with DDAF and salicylaldehyde. (b) UV-Vis spectra of Model 1 and its monomers in DMF.

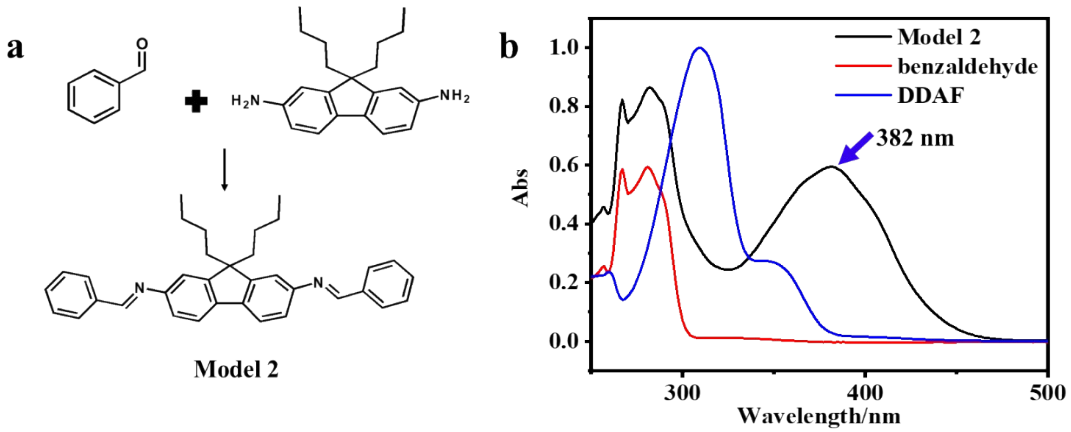

Figure S26. (a) Synthesis of Model 2 with DDAF and benzaldehyde. (b) UV-Vis spectra of Model 2 and its monomers in DMF.

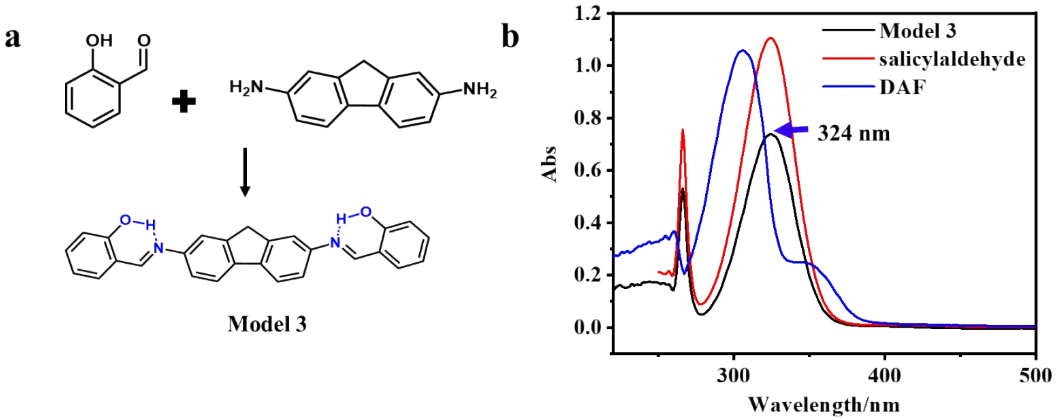

Figure S27. (a) Synthesis of Model 3 with DAF and salicylaldehyde. (b) UV-Vis spectra of Model 3 and its monomers in DMF.

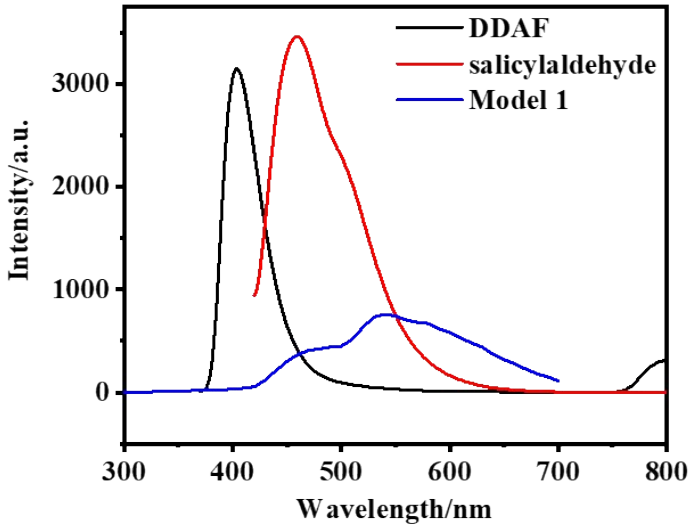

Figure S28. Fluoresce spectra of Model 1, DDAF, and salicylaldehyde in DMF.

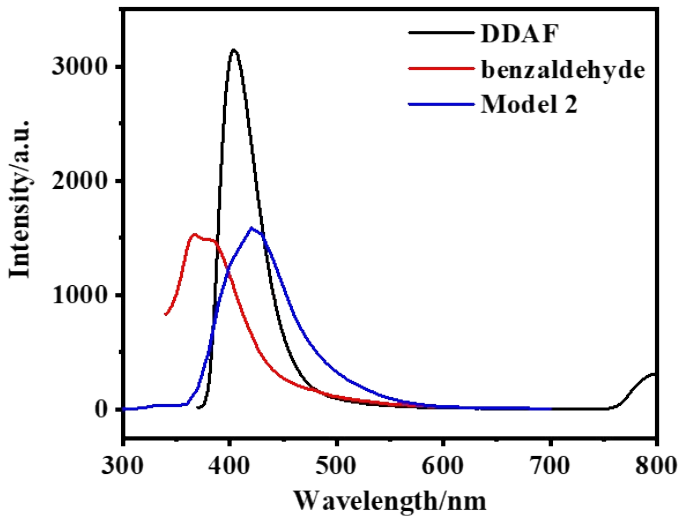

Figure S29. Fluoresce spectra of Model 2, DDAF, and benzaldehyde in DMF.

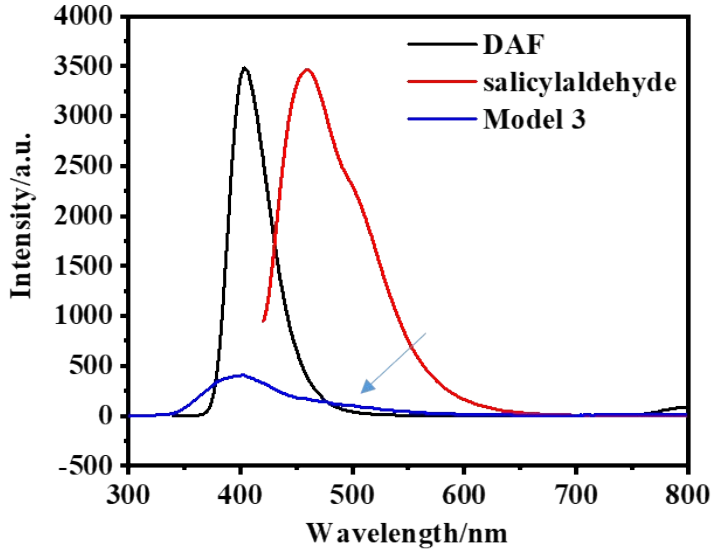

Figure S30. Fluoresce spectra of Model 3, DAF, and salicylaldehyde in DMF. (The arrow shows the weak ESIPT emission from Model 3)

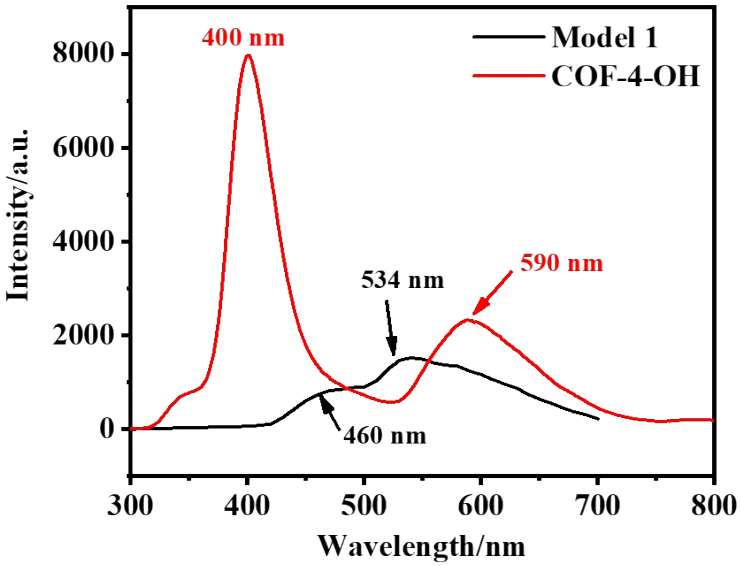

Figure S31. Fluorescence profiles of COF-4-OH and Model 1 in DMF at 0.05 mg mL^{-1} level.

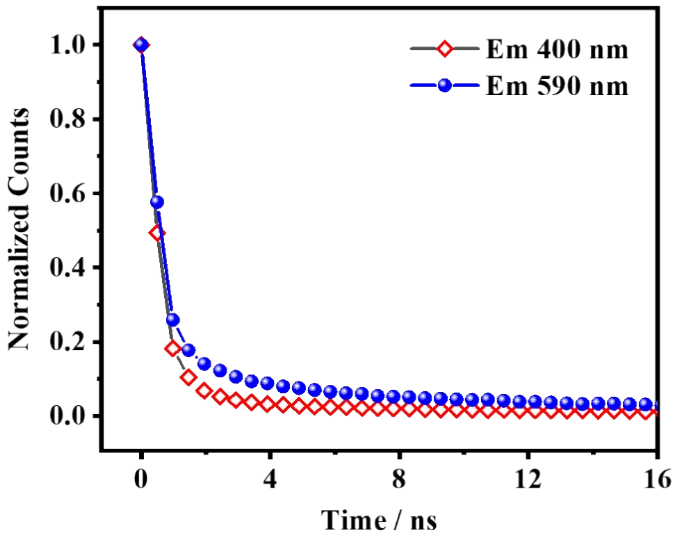

Figure S32. The fluorescence lifetime of the emissions at 400 and 590 nm from COF-4-OH in DMF.

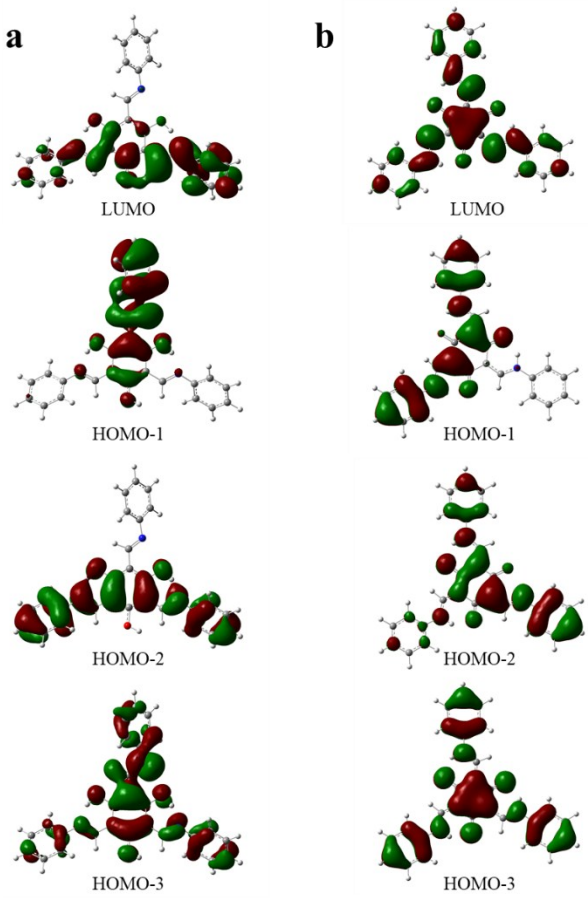

Figure S33. HOMO-LUMO energy diagram of COF-4-OH fragment (a) enol state (b) keto state obtained from time dependent density functional theory (TD-DFT).

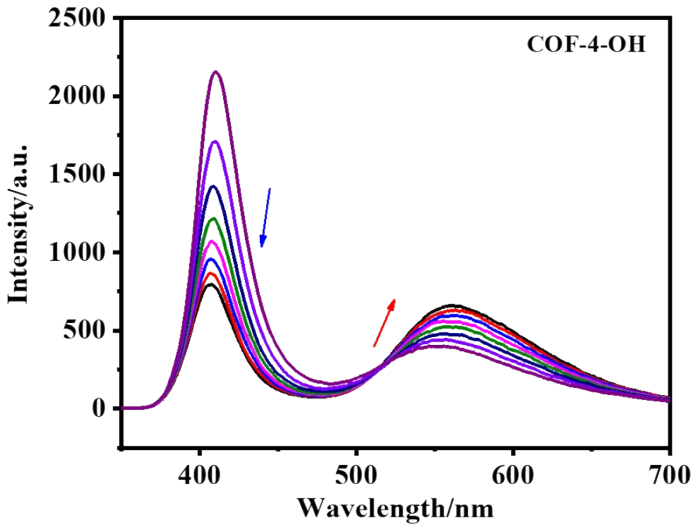

Figure S34. Fluorescence evolution of COF-4-OH along with the synthesis time from 0 to 60 min (with 1,4-dioxane as the solvent). With the gradual formation of COF-4-OH, the blue emission blue-shifted and the red emission red-shifted as the important property of ESIPT effect.

To illustrate the ratiometric fluorescence detection without disturbing of concentration and environment, we chose lower COF-4-OH concentration to detect the water content. Both the higher and lower COF-4-OH concentration shows the same intensity ratio between the emissions at 400 and 590 nm.

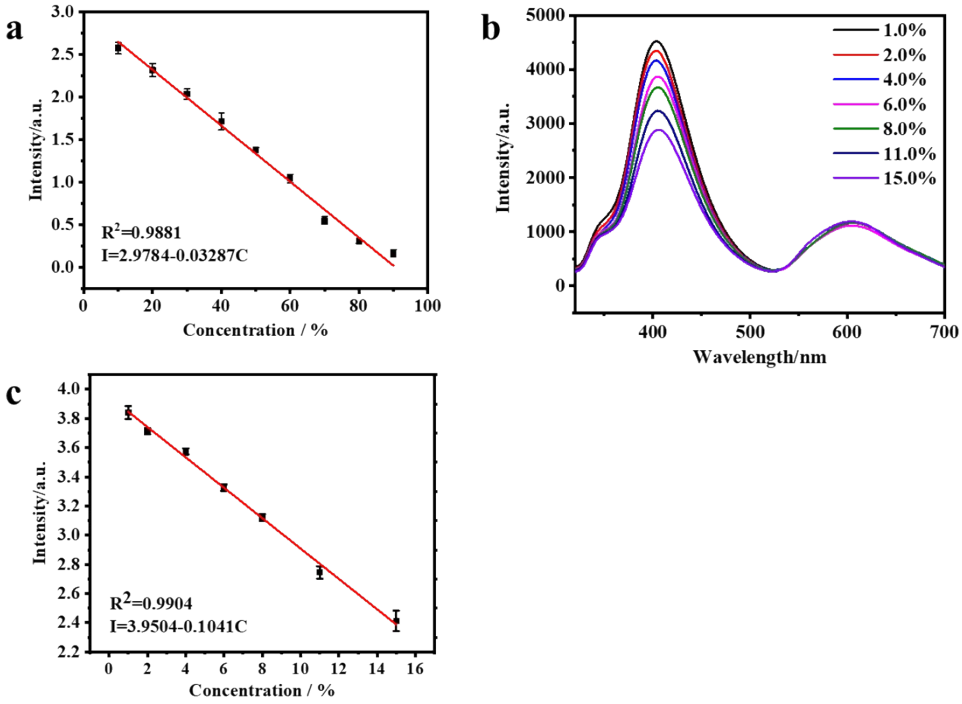

Figure S35. (a) The fitting curve between fluorescence intensity and water content from 10% to 90% in ethanol. (b) COF-4-OH response to water content from 1.0% to 15.0% (0.025 mg mL^{-1}). (c) The fitting curve between luminescence intensity and water content from 1.0% to 15.0% in ethanol.

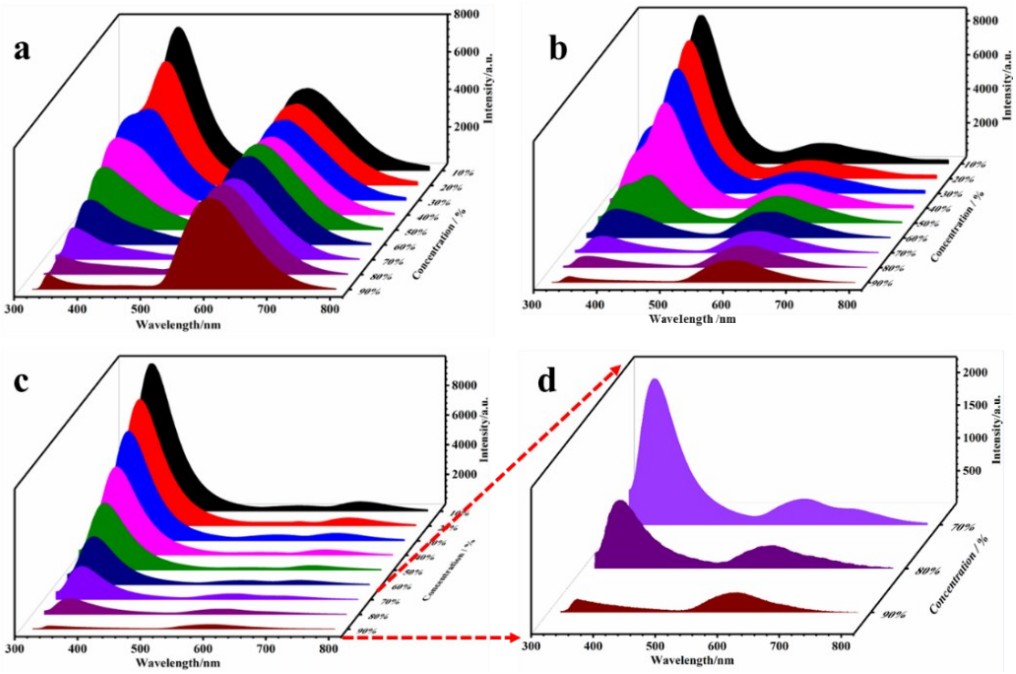

Figure S36. Fluorescence profiles of COF-4-OH in (a) methanol, (b) N,N-dimethylformamide, and (c) dimethyl sulfoxide (DMSO) containing different water contents. (d) Fluorescence profiles of COF-4-OH in DMSO containing 70%, 80%, and 90% water contents. The emission at 400 nm is so high that the emission at 590 nm is difficult to identify. The profiles were therefore enlarged to reveal the ratiometric fluorescence detection.

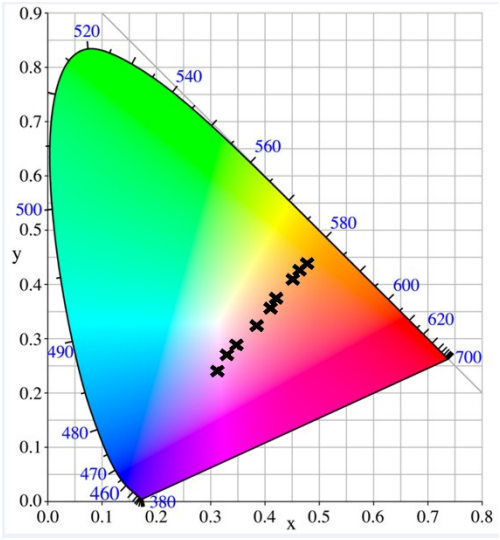

Figure S37. CIE coordination responding to different pH for COF-4-OH (from left to right: pH from 8.0 to 4.0) to reveal the potential for visible detection of pH.

Table S1. The main emissions and quantum yield of the COFs in solid states and three models in solution states.

	Emission (nm)	QY (%)
COF-0	--	0
COF-4	395	0.1±0.001
COF-0-OH	375, 525	0.3±0.003
COF-4-OH	400, 590	10.7±0.003
COF-8-OH	365, 570	3.1±0.011
Model 1	460, 534	4.6±0.013
Model 2	430	3.5±0.010
Model 3	400, 490	1.6±0.010

Support Reference:

1. L. Wang, B. Dong, R. Ge, F. Jiang and J. Xu, *ACS Appl. Mater. Interfaces*, 2017, **9**, 7108-7114.